

# CRACK DETECTION IN WELDED MECHANICAL STRUCTURES USING COUPLED VIBRATIONS

D. Liu<sup>1,2</sup>, H. Gurgenci<sup>1,2</sup> and M. Veidt<sup>2</sup>

<sup>1</sup>CRCMining, 2436 Moggill Road, Pinjarra Hills, QLD 4069, Australia

<sup>2</sup>Department of Mechanical Engineering, The University of Queensland, QLD 4072, Australia

**Abstract:** Detection of a fatigue crack in a welded frame structure is studied in this paper using coupled response measurements. Similarity to real engineering structures is maintained in the fabrication of the test frame with hollow section chords and branch members. The fatigue crack was created by a special reciprocating mechanism that generates cyclic stress on a beam member of the structure. The methodology of coupled response measurements is first demonstrated on a single hollow section beam by analytical simulation and experimental validation. The issues of using this approach for fatigue crack detection in real structures are then examined. Finally, the experimental results of the frame under different scenarios are presented. The existence of the crack is clearly observable from the FRF plots. It is suggested that this approach offers the potential to detect cracks in welded frame structures and is a useful tool for routine maintenance work and health assessment.

## 1. INTRODUCTION

Fatigue cracks in welded structures are of serious concern to both industrial and engineering communities. Early detection of cracks is important to optimize productivity, reduce maintenance cost and prevent catastrophic failures. Vibration based damage detection methods offer an effective, inexpensive and fast tool for nondestructive testing. They are based on the fact that any structural change due to damage should manifest itself as changes in the structure's dynamic characteristics. Because of its potential for structural damage detection, monitoring the changes in the vibration characteristics of a structure has been a popular research topic during the past several decades.

Reviews on vibration of damaged structures were reported by Dimarogonas [1] and Doebling et al [2]. Many identification techniques have been proposed based on different system parameters. Some authors used the change of natural frequencies [3-4] or mode shapes [5-6] as the indicator of damage while others detected structural damage directly from dynamic response in time domain or from Frequency Response Functions (FRF)[7]. Despite a certain degree of success with these techniques, a common observation derived from the above studies is the relative insensitivity of global parameters such as mode shapes and frequencies to local damage.

An alternative option is offered through coupled response measurements. In the present investigation coupled response refers to the ability of a cracked structural member to experience composite vibration modes (axial and bending) when excited purely laterally. Dimarogonas and Paipetis introduced the coupling effect due to a crack by using a local flexibility matrix to model the cracked cross section of a shaft [8]. Papadopoulos et al studied coupled vibration on a cracked shaft under a few different configurations [9-11]. But the available results were mostly based on the analytical

simulation and only solid section structures were considered. It is of great interest to demonstrate the use of coupled response measurements to detect cracks in real field applications. As the first step earlier research by the authors demonstrated the experimental feasibility of the methodology on a circular hollow sections (CHS) beam [12]. The success of the technique on an isolated beam does not necessarily imply that it is a valid proposal for damage detection in structures. Firstly, most of damage types in real structure are fatigue cracks and a fatigue crack is different from an artificial crack created by a hacksaw. Secondly, on a structure with many members, the local modes of vibration are typically superimposed on large amplitude global modes and there are strong interactions between global modes and the modes on the adjacent members. In spite of these effects, it was hypothesized that, since the technique did not depend on accurate identification of the mode shapes, it had the potential to detect damage on beams that are not subject to ideal boundary conditions but are members in larger structures. This paper addresses these issues and presents the recent results on a welded frame structure.

Frame-like structures with hollow-section members are very popular in engineering applications. Such structures are typically made of chord members cross-connected by smaller branches also known as lacings. A test rig simulating such a welded structure was fabricated and fatigue cracks were created by a special mechanism. Vibration experiments were conducted on the structure with and without fatigue cracks. This paper first introduces the methodology of coupled response measurements through a summary of analytical and experimental research on a single beam. The fabrication of a welded frame structure and the mechanism to generate fatigue cracks are then presented. The experimental set-up, the testing procedures, and the various crack cases are also included. Finally the testing results on the structure are summarized to demonstrate the feasibility of this approach.

## 2. CRACK DETECTION METHODOLOGY OF COUPLED RESPONSE MEASUREMENTS FOR CHS BEAM

In this section, the vibration characteristics of a cracked beam member is studied. It shows that the lateral FRFs of the cracked beam differ from the uncracked one by the presence of extra new peaks corresponding to axial modes. This coupling property is analytically demonstrated through traditional beam theory and fracture mechanics approach. Experiments conducted on a beam are used to validate this method.

### 2.1 Local flexibility matrix and axial-bending coupling coefficients of a CHS member

A crack in a structural member introduces additional local flexibility, which is affected by the crack severity and location. The extra flexibility changes the dynamic behavior of the system. The dynamic influence of the crack manifests itself as coupled vibration modes (for example, axial and bending) under purely lateral excitation. This phenomenon can be observed through the appearance of extra new peaks on the FRF plots.

The key step to explain this phenomenon is to analyze the dynamical behavior of a cracked beam section and establish the local stiffness or flexibility matrix of the cracked member under general loading. In general, the local flexibility of a beam at any single point can be described by inserting a virtual joint at that point and representing that joint by a local flexibility matrix. The matrix size is  $6 \times 6$  namely three translational and three rotational components. The coordinate system and the corresponding generalized forces are shown in Figure 1. Here subscript 1 is used for the longitudinal force, 2 and 3 for the shearing forces, 4 and 5 for the bending moments and 6 for the torsional moment. Using the local flexibility matrix, the extra displacement along any degree of freedom due to the presence of the crack is given by the following equation:

$$\{u\} = [C]\{P\} \quad (1)$$

Where  $\{u\}$ ,  $[C]$  and  $\{P\}$  are displacement vector, local flexibility matrix and force vector, respectively with  $\{u\} \in R^{6 \times 1}$ ,  $[C] \in R^{6 \times 6}$ ,  $\{P\} \in R^{6 \times 1}$ .

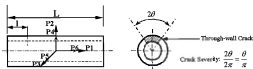


Figure 1. CHS beam under general loading and the description of crack severity

The displacement due to the presence of the crack is computed using Castigliano's theorem. It can be expressed as the function of the loading forces. The local flexibility matrix is then constructed through equation (1). The general expression for its matrix elements can be written in the following form [8]:

$$c_{ij} = \frac{1}{E'} \iint_A \left[ \frac{\partial^2}{\partial P_i \partial P_j} \sum_{m=1}^{III} e_m \left( \sum_{n=1}^6 K_{mn} \right) \right]^2 dA \quad (2)$$

Where  $E' = E$  for plane stress,  $E' = E/(1 - \nu^2)$  for plane strain,  $\alpha = 1 + \nu$ ,  $E$  and  $\nu$  are Young's modulus and Poisson's ratio, respectively,  $e_m = 1$  for  $m = I, II$  and  $e_m = \alpha$  for  $m = III$ ,  $K_{mn}$  is the stress intensity factor of mode  $m$  ( $m = I, II, III$ ) due to the load  $P_n$  ( $n = 1, 2, \dots, 6$ ),  $A_c$  represents the cracked area.

Expression (2) can be further manipulated as:

$$c_{ij} = \frac{2}{E'} \iint_{A_c} \left[ \frac{\partial K_{ij}}{\partial P_i} \frac{\partial K_{ij}}{\partial P_j} + \frac{\partial K_{ij}}{\partial P_i} \frac{\partial K_{ij}}{\partial P_j} + \alpha \frac{\partial K_{ij}}{\partial P_i} \frac{\partial K_{ij}}{\partial P_j} \right] dA \quad (3)$$

It is clear that the local flexibility matrix is determined by the relevant stress intensity factors. From the expression one can judge whether or not the value of  $c_{ij}$  is nonzero. Mathematically, if  $K_{mi} \neq 0 \cap K_{mj} \neq 0$  ( $m$  is either one of the fracture mode  $I, II$  or  $III$ ) then in most cases  $c_{ij} \neq 0$ . Physically,  $P_i$  if  $P_j$  and contribute to the same fracture mode, either opening, sliding or out-of-plane shear mode, then coupling between the  $i^{\text{th}}$  and  $j^{\text{th}}$  DOF will exist. In practice this principle helps to make predictions about which DOFs are coupled even though the accurate stress intensity factors are not available. For example, for a beam with a cross sectional crack, both axial force and bending moment tend to open the crack (mode  $I$ ). This indicates the axial-bending coupling is expected.

In this study, the focus is on circumferential cracks encountered in CHS (Circular Hollow Section) beams. One of the common crack types is a so-called through-wall crack which is propagated through the entire wall thickness. The severity is represented by the ratio of the crack area to the total cross-sectional area as shown in Figure 1. In the figure the shaded area indicates the cracked part of the cross-section. For example, a 10%-crack represents the loss of 10% of the cross-sectional area of the beam. For other types of cross section or different crack configurations the stress intensity factor formulations will change but the methodology remains the same.

For circumferential through-wall cracks the solutions of the stress intensity factors are given below [13]:

Axial force  $P_1$ :

$$K_{I1} = \frac{P_1}{2\pi R t} \sqrt{\pi R \theta} \left\{ 1 + A_1 \left[ 5.3303 \left( \frac{\theta}{\pi} \right)^{1.5} + 18.773 \left( \frac{\theta}{\pi} \right)^{4.24} \right] \right\} \quad (4)$$

Where  $R = (R_o + R_i)/2$  is the mean radius,  $t$  is wall thickness and  $\theta$  is the half angle of the total through-wall crack (the crack severity is indicated by  $\theta/\pi$  as percentage as shown in Figure 1) and  $A_1$  is determined by:

$$A_1 = \begin{cases} \left( 0.125 \frac{R}{t} - 0.25 \right)^{0.25} & \text{if } 5 \leq \frac{R}{t} \leq 10, \\ \left( 0.4 \frac{R}{t} - 3.0 \right)^{0.25} & \text{if } 10 \leq \frac{R}{t} \leq 20 \end{cases} \quad (5)$$

Bending moment  $P_3$ :

$$K_{33} = \frac{P_3}{\pi R^2 t} \sqrt{\pi R \theta} \left[ 1 + A_1 \left[ 4.5967 \left( \frac{\theta}{\pi} \right)^{1.5} + 2.6422 \left( \frac{\theta}{\pi} \right)^{4.24} \right] \right] \quad (6)$$

And  $A_1$  is same as expression (5).

Substituting the  $K_{11}$  and  $K_{33}$  into equation (2) yields the matrix entries  $c_j$  by analytical or numerical integration. Since the wall thickness  $t$  is a constant, the integration is carried out over the crack angle  $2\theta$  defined in Figure 1. Once the local flexibility matrix is obtained, the vibration modes and FRFs of a cracked CHS beam can be developed using classical beam theory.

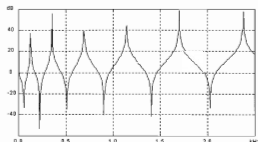
## 2.2 Simulation results on a single CHS beam

For clarity, the method will first be demonstrated on a single beam. A free-free beam is used to facilitate ready comparison between analytical and experimental results without having to include the effect of the boundary conditions. Later on, results will be presented for a beam that is part of a large structure. The following parameters apply to the free-free tests: beam length 1.5 m, outside diameter 48.3 mm, wall thickness 3.2 mm, Young's modulus 200GPa and a mass density of 7850 kg/m. The damage is located at a distance of 0.45m (30% of total length) from one end.

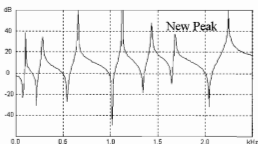
The calculated driving point FRFs of a free end of the beam are shown in Figure 2. Plot (a) is the lateral FRF for an undamaged beam, i.e. both the excitation and the measurements are in a plane perpendicular to the beam axis. For an undamaged beam, no axial movement should be expected. The peaks shown in Figure 2(a) all correspond to bending modes. Plot (b) shows the lateral FRF when the damage is introduced. The damaged section is treated as a special boundary and its mathematical model is described by the local flexibility matrix. Because of the nonzero off-diagonal term  $c_{13}$ , the analytical solution shows that axial modes can be observed in lateral FRFs. Comparing plots (b) against (a), one observes that the presence of the crack influences the FRFs in two ways: (i) all natural frequencies are slightly reduced because of loss of stiffness at the crack location; and (ii) an extra peak is introduced as noted on the plots. The natural frequency (1680 Hz) corresponding to the new peak is close to the undamaged axial natural frequency (1682 Hz). This indicates a coupling of lateral and axial vibrations.

## 2.3 Experimental results on the CHS beam

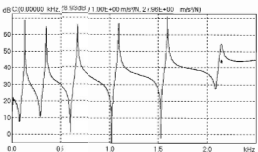
In order to determine the practical feasibility of this approach, it has to be demonstrated that the mode coupling is clearly observable not only in analytical simulations but also on experimental FRFs. Modal tests were conducted for a CHS beam with the dimensions listed above. The beam was suspended by a pair of soft elastic straps simulating free-free boundary conditions. The artificial crack was created using a 0.5mm thickness hacksaw and at the same location as in the analytical case. The beam was excited with an impulse hammer. This provided excitation covering a frequency range up to 2500 Hz. The responses were measured at the free end



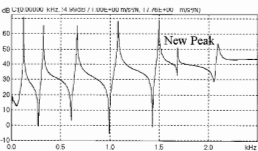
(a) FRF of undamaged CHS beam (Analytical)



(b) FRF of damaged CHS beam (Analytical)



(c) FRF of undamaged CHS beam (Experimental)



(d) FRF of damaged CHS beam (Experimental)

Figure 2. Comparison of analytical and experimental FRFs of undamaged and damaged CHS beam

close to the cracked cross-section while the position of the excitation point was evenly chosen along the beam. The data acquisition and FFT analysis were implemented by the OR24 analyzer. This is an integrated 4-ch modal testing and analysis tool featuring multiple trigger mode, FRF displaying and flexible data storage format. The FRFs were calculated from input and output data using standard H1 estimation [14]. A laptop computer was used as an interface for data acquisition and analysis.

Both undamaged and damaged CHS beams were tested and the corresponding FRFs and modal shapes were generated. The bottom parts of Figure 2 show the driving point FRFs for one free end of the undamaged and damaged beam. The extra new peak is clearly observable in both cases. Since the current analytical model does not consider damping, the relative peak magnitudes and the modal damping are slightly different as can be seen from Figure 2. However, for the purpose of this study, the basis of comparison between the plots is the locations of the peaks along the frequency axis not their amplitudes. On this basis, there is strong similarity between the two figure sets. It is essential to note the good agreement between the measured and the predicted frequencies for the uncracked beam. The amount of shift caused by the introduction of the damage is also similar between the two sets. The similarity between the experimental and analytical results displayed in Figure 2 supports the statement that a coupled response analysis is a valid approach to damage detection in beams. The detailed frequency data are not included here since the focus in our approach is on introduction of a coupled mode rather than the frequency reduction information.

The analytical and experimental results on a single beam suggest that the vibration mode coupling can be used as a damage detection tool by using the presence of extra new peaks in FRF plots. However, for field applications more realistic issues need to be addressed such as the difference between fatigue cracks and saw cuts. The following section addresses these issues.

### 3. FABRICATION OF A WELDED FRAME STRUCTURE AND GENERATION OF A FATIGUE CRACK ON A JOINT

A frame-like test rig was fabricated to represent a typical engineering structure. The rig was constructed of hollow section mild steel beams, using square sections as main base and circular sections as the test specimen. As shown in Figure 3, the overall dimension of the structure is 1.5m x 1.5m in plan and 0.9m in height. The cross sectional size of the base members is 125mm x 125mm with wall thickness 9mm. The outside diameter of the chord member and the test specimen is 114.3 mm with wall thickness 4.5mm and 48.3 mm with wall thickness 3.2mm, respectively.

The test rig serves two basic functions: the first is to create fatigue cracks on the joint of the chord and branch members and the second is to provide vibration test rig to investigate the feasibility of crack detection using coupled response measurement methodology.

The cyclic stress in the testing beam member is generated by a reciprocating-bending mechanism. An eccentric shaft is driven by the AC motor applying a bending load on the beam by the reciprocating motion of a connecting rod. The mean stress and the amplitude are controlled by the connecting rod pretension and the eccentric distance of the driving shaft, respectively. As a safety feature, a limit switch is used to turn off the power of the AC motor when either end of the test beam is broken. The number of loading cycles is displayed on a LCD panel. The fatigue crack is formed on the welding joint of beam and the chord member.

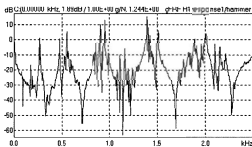
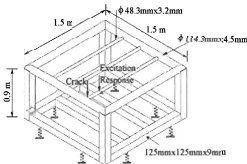


Figure 3. Schematic drawing of the welded frame structure and a FRF shown on broad band frequency

### 4. EXPERIMENTAL RESULTS OF THE WELDED FRAME STRUCTURE

The frame is supported by eight pieces of rubber pads simulating free-free boundary condition. The location of response and impact point is 0.15m (1/10th of the beam length) away from the crack. However, the choices of response and excitation points are not limited to certain locations since the extra peaks generally manifest themselves on other FRFs as well.

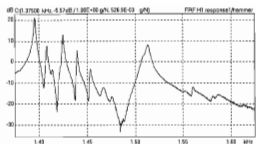
Although the crack detection methodology is similar to the single beam cases the new issue arising from the frame tests is the selection of the frequency range to present the FRFs. Figure 3 shows one of the FRF plots with the same frequency range as the single beam test discussed previously. There are a large number of closely spaced resonance peaks in the FRF plot compared to the single beam case. It is not practically

possible to confidently distinguish the extra peak from the others. In order to obtain more detailed description in the local frequency domain the zoom analysis was used to increase the frequency resolution while maintaining the desired baseband frequency [14]. The zoom process is a well-known technique in frequency analysis and it is provided as a built-in function in the OR24 analyzer and the frequency range can be selected according to the anticipated frequency band.

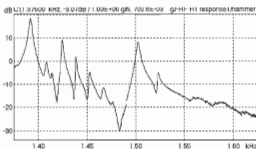
The observation of the single beam experiments shows that the frequency of the extra new peak is close to the longitudinal natural frequency of the beam. This can be used as a guidance to select the desired frequency regime to observe the new peaks. In this case, for the same size beam as in the test frame its analytical longitudinal first natural frequency for ideal fixed-fixed boundary condition is 1682 Hz. Considering the flexibility of the welding joints to the beam the actual longitudinal first natural frequency is approximately 1525 Hz. The frequency range is finally selected from 1375 to 1625 Hz. The experimental lateral driving point FRFs of point A for uncracked and cracked cases are presented in Figure 4 as plot (a) and plot (b), respectively. Comparing the two plots, the following features distinguish the cracked case from the uncracked one: (1) there are extra peak(s) on FRF plot (b); (2) the natural frequency corresponding to the new peak is close to the axial natural frequency of the undamaged beam. The new peak was caused by the crack through a mechanism similar to what was observed on the isolated beam. On the isolated beam, it was possible to rigorously demonstrate that the extra peak was produced by a coupled mode that owed its existence to the presence of the crack by analyzing the mode shapes [12]. On a beam tested as part of a larger structure, the local mode shapes are superimposed on large-amplitude global mode shapes and it may not be possible to separate between the local and global modes without performing a comprehensive modal test on the entire structure. This is not feasible in most engineering circumstances. However, our present results show that in-situ damage detection is possible and feasible with the proposed method because the introduction of the new peak is sufficient evidence for crack presence and knowledge of the local or global mode shapes is not required.

## 5. COMMENTS AND CONCLUSIONS

This paper reports the results of the coupled response measurement crack detection method obtained in tests on a welded frame structure containing hairline fatigue cracks. The method works by detecting the emergence of a new coupled mode in FRFs produced by unidirectional excitation. The methodology was first introduced and demonstrated on a free-free CHS beam by both analytical simulation and experimental confirmation. In each case the undamaged and damaged beam were studied. The results suggest that the coupling property between the longitudinal and lateral vibration is a good indicator of the existence of a crack. The



(a) FRF of uncracked frame



(b) FRF of cracked frame

Figure 4. Experimental FRFs of uncracked and cracked frame structure

coupling modes normally can be observed through the extra peaks appearing on the driving point FRFs.

In the second stage this method was applied to real structures for real cracks. As a representation of popular welded structures a frame-like test rig was constructed. A hairline fatigue crack was created on the welded joint by repetitive cycling loading of the beam member. The experimental FRFs of the beam were obtained for intact and cracked scenarios using the same modal test techniques. The results show that distinguishable new peaks appear on FRF plots when fatigue crack is present.

The application of coupled-response method to real-like structures has specific issues that are addressed in this paper the first time in literature. Most mechanical structures are made of several main chords connected by lacing members and, in such configurations, it is not uncommon for the local modes to lie close to global modes. In addition to this, since these are lightly-damped structures, the local modes for the adjoining members interact with the modes of the test member. Because of these difficulties, there has been no report to date of an experimental study with successful identification of a fatigue crack using a coupled-response method on a reasonably complicated structure.

Although the results presented in the paper were obtained on laboratory environment the principle observed in the investigation gives valuable insights to on site field applications.

## REFERENCES

- [1] Dimarogonas A.D. (1996) Vibration of cracked structures: a state of the art review. *Engineering Fracture Mechanics*, **55**(5), 831-857.
- [2] Doebbling S.W., et al (1996) Damage identification and health monitoring of structural and mechanical systems from changes in their vibration characteristics; a literature review. *Los Alamos National Laboratory report, LA-13070-MS*.
- [3] Silva J. M. & Gomes A. (1990) Experimental dynamic analysis of cracked free-free beam. *Experimental Mechanics*, **30**(1), 20-25.
- [4] Lee Y.S. & Chung M.J. (2000) A study on crack detection using eigenfrequency test data. *Computer & Structures*, **77**(3), 327-342.
- [5] Rizos P.F. & Aspragathos N. (1990) Identification of crack location and magnitude in a cantilever beam from the vibration modes. *Journal of sound and vibration*, **138**(3), 381-388.
- [6] Pandey A.F., Biswas M. & Samman M.M. (1991) Damage detection from changes in curvature mode shapes. *Journal of sound and vibration*, **145**, 321-332.
- [7] Springer W. T., Lawrence K. L. & Lawley T. J. (1988) Damage assessment based on the structural Frequency Response Function. *Experimental Mechanics*, **28**(1), 34-37.
- [8] Dimarogonas A. D. & Paipetis S. A. (1983) *Analytical Methods in Rotor Dynamics*. New York: Applied Science Publishers.
- [9] Papadopoulos C.A. & Dimarogonas A.D. (1987) Coupled longitudinal and bending vibrations of a rotating shaft with an open crack. *Journal of sound and vibration*, **117**, 81-93.
- [10] Papadopoulos C.A. & Dimarogonas A.D. (1992) Coupled vibration of cracked shafts. *Journal of sound and vibration*, **114**, 461-467.
- [11] Gounaris G.D. & Papadopoulos C.A. (2002) Crack identification in rotating shafts by coupled response measurements. *Engineering Fracture Mechanics*, **69**, 339-352.
- [12] Liu D., Gurgenci H. & Veidt M. (2003) Crack detection in hollow section structures through coupled response measurements. *Journal of sound and vibration*, **261**, 17-29.
- [13] Anderson T. L. (1994) *Fracture Mechanics: Fundamentals and Applications*. Boca Raton: CRC Press.
- [14] McConnell K.G. (1995) *Vibration Testing: Theory and Practice*. New York: John Wiley.

## ACKNOWLEDGMENTS

The authors would like to thank the CRC Mining and the Department of Mechanical Engineering of the University of Queensland for their support of this project.

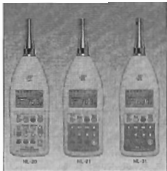


# ARL Sales & Hire RION

Noise, Vibration & Weather Loggers

Sound & Vibration Measuring Instruments

New EL-316 Type 1 Noise Logger  
New EL-315 Type 2 Noise Logger  
Push button programming menu  
Enlarged memory  
Fixed post microphones  
Overload indicator  
Trigger functions  
Optional mobile modem



New generation of Rion meters  
NL-20 Type 2 sound level meter  
NL-21 Type 2 sound level meter  
NL-31 Type 1 sound level meter  
Comply with IEC61672-1 standard  
Measure and store percentile statistics  
Optional memory card for data transfer  
Optional filter card for frequency analysis

## Acoustic Research Laboratories

Proprietary Limited

A.B.N. 47 050 100 804

Noise and Vibration Monitoring Instrumentation for Industry and the Environment

A **SOUND THINKING GROUP** Company



Reg. Lab 14172  
Acoustics & Vibration  
Measurement

ARL Sydney: (02) 9484-0800 Occupational Safety Services Melbourne: (03) 9897-4711  
Pierce Calibration Laboratory Perth: (08) 9356 7999 Wavecon Adelaide: (08) 8331-8892 Bekur Brisbane: (07) 3820 2488